Journal of Solid State Chemistry **150,** 139–144 (2000)
doi:10.1006/jssc.1999.8567, available online at http://www.idealibrary.com on IDEAL®

Ce_2Ni_2Cd—A New Intermediate-Valent Cerium Compound

Dirk Niepmann, Rainer Pöttgen,[1] Bernd Künnen, and Gunter Kotzyba

Anorganisch-Chemisches Institut, Universität Münster, Wilhelm-Klemm-Straße 8, D-48149 Münster, Germany

Received September 7, 1999; in revised form November 2, 1999; accepted November 5, 1999

Ce_2Ni_2Cd was synthesized by reacting the elements in a sealed tantalum tube using a high-frequency furnace with a water-cooled sample chamber. The structure was refined from single-crystal X-ray data: ordered U_3Si_2 type, *P4/mbm*, $a = 755.67(8)$ pm, $c = 375.14(6)$ pm, w$R2 = 0.0408$, 232 F^2 values, and 13 parameters. A refinement of the occupancy parameters showed defects on the nickel site, resulting in a composition of $Ce_2Ni_{1.88(1)}Cd$ for the crystal investigated. The structure may be described as an intergrowth of CsCl and AlB_2 related slabs of compositions *CeCd* and $CeNi_2$. Magnetic susceptibility measurements indicate intermediate-valent behavior of the cerium atoms. The susceptibility data can be fit to a modified Curie–Weiss expression with $\Theta_P = -5.2(2)$ K, $\mu_{exp} = 0.79(3)\ \mu_B$/Ce, and a temperature-independent contribution $\chi_0 = 67.5(7) \times 10^{-9}$ m^3/mol. Temperature-dependent resistivity measurements indicate metallic behavior with a specific resistivity of 140 $\pm$ 20 μΩ cm at room temperature. Below 50 K the specific resistivity reveals a T^2 dependence with $\rho_0 = 84.4(1)$ μΩ cm and $A = 0.0056(1)$ (μΩ cm)/K^2.

Key Words: **intermetallic cerium compounds; crystal structure; intermediate valency.**

INTRODUCTION

In recent years the large family of ternary intermetallic R_2T_2X compounds (R = actinoid or rare earth metal; T = transition metal; X = In, Sn) has been intensively investigated with respect to the greatly varying physical properties (1–7, and references therein). Besides intensive experimental investigations, also studies about the chemical bonding in these fascinating materials have been performed (8–11, and references therein). The magnetic properties of the actinoid and cerium-containing R_2T_2X compounds vary from nonmagnetic ground states to Kondo, heavy-fermion, or spin-fluctuating systems. Most of the uranium-containing indides and stannides exhibit at low temperatures a strong enhancement in the electronic coefficient of the specific heat supporting their classification as heavy-fermion systems (12).

[1] To whom correspondence should be addressed. E-mail: pottgen@uni-muenster.de.

Most of the R_2T_2X compounds crystallize with the tetragonal Mo_2FeB_2-type structure (13), a ternary ordered version of the U_3Si_2 type (14, 15). In some cases the formation of superstructures was observed (16–18). Those compounds crystallize with the Er_2Au_2Sn type (16), a ternary ordered version of the Zr_3Al_2 type (19). According to electronic structure calculations (11), the occurence of the superstructure is most likely due to packing reasons.

The indides and stannides are easily accessible via arc-melting techniques also in quantities of several grams for neutron diffraction experiments. This preparation method, however, is not applicable when elements with low boiling points are used. A large weight loss would occur during the arc-melting procedure. We have now extended our investigations of the R_2T_2X compounds with respect to cadmium as the X component. Due to its very low boiling point of 1040 K, quantitative syntheses are only possible in closed systems. We have modified the synthesis conditions and prepared such cadmium compounds in sealed tantalum tubes in a high-frequency furnace. Herein, we report on the synthesis and structure refinement of metallic intermediate-valent Ce_2Ni_2Cd, the first cadmium compound in the series of tetragonal R_2T_2X intermetallics.

EXPERIMENTAL

Starting materials for the synthesis of Ce_2Ni_2Cd were ingots of cerium (Johnson Matthey), nickel wire (Johnson Matthey, ∅ 0.38 mm), and a cadmium rod (Johnson Matthey, ∅ 8 mm), all with stated purities better than 99.9%. The larger cerium ingots were first cut into smaller pieces under paraffin oil. The latter was washed away with *n*-hexane. Both liquids were dried over sodium wire. The cerium pieces were kept in Schlenk tubes under vacuum.

In the first step, the small cerium pieces were arc-melted to buttons under argon in a miniaturized arc-melting apparatus. The argon was purified before over titanium sponge (900 K), silica gel, and molecular sieves. Details about the arc-melting apparatus are given in Ref. (20). The cerium button (about 500 mg) was then mixed with the nickel wire and cadmium pieces in the ideal 2:2:1 atomic ratio and

0022-4596/00 $35.00

sealed in a small-sized tantalum tube (about 1 cm^3 tube volume). The tube was placed in a water-cooled quartz glass sample chamber in a high-frequency furnace (Kontron Roto-Melt, 1.2 kW) and first heated with the maximum power output of the high-frequency generator. The experimental setup is described in detail in Ref. (21).

The exothermic reaction was easily visibly by the occurrence of white heat for about 1 s. The annealing temperature was then lowered to about 1100 K four about 1 min and then raised again to the maximum. Subsequently, the tube was annealed for 1 h at about 900 K. The reaction resulted in a brass-yellow polycrystalline sample of Ce_2Ni_2Cd which could easily be separated from the tantalum tube.

The sample was analyzed by EDX measurements using a Leica 420 I scanning electron microscope with CeO_2, Ni, and Cd as standards. No impurity elements heavier than sodium were detected and the analyses (40 ± 2 at.% Ce; 41 ± 2 at.% Ni; 19 ± 2 at.% Cd) were in good agreement with the ideal composition. The standard deviations account for the various analyses obtained for different crystallites. Tantalum contaminations from the container material could thus be safely ruled out.

Ce_2Ni_2Cd was characterized through a Guinier powder pattern which was recorded with Cu$K\alpha_1$ radiation using α-quartz ($a = 491.30$ pm; $c = 540.46$ pm) as an internal standard. The pattern could completely be indexed with a primitive tetragonal cell. The Guinier powder data are listed in Table 1. The lattice constants (see Table 2) were obtained from a least-squares fit of the Guinier data. To assure correct indexing, the observed pattern was compared with a calculated one (22), taking the atomic positions from the structure refinement. The lattice constants of the single crystal ($a = 755.8(1)$ pm; $c = 374.9(1)$ pm) were in good agreement with the powder data.

TABLE 1
Guinier Powder Data (Cu$K\alpha_1$ Radiation) for Ce_2Ni_2Cd

h	k	l	$2\theta_0$	d_c (Å)	d_o (Å)	I_c	I_o
2	0	0	23.55	3.7784	3.7743	1	vw
0	0	1	23.70	3.7514	3.7508	1	vw
2	1	0	26.36	3.3795	3.3781	22	m
1	1	1	29.06	3.0703	3.0702	16	w
2	2	0	33.48	2.6717	2.6745	18	w
2	0	1	33.62	2.6621	2.6636	63	s
2	1	1	35.75	2.5109	2.5097	100	vs
3	1	0	37.60	2.3897	2.3904	51	s
3	2	0	43.12	2.0959	2.0960	5	w
3	1	1	44.92	2.0155	2.0161	2	vw
0	0	2	48.47	1.8757	1.8765	18	w
4	1	0	49.69	1.8328	1.8333	16	w
3	3	0	51.24	1.7811	1.7814	5	w
4	2	0	54.25	1.6897	1.6895	6	w
4	1	1	55.78	1.6468	1.6467	21	m
2	1	2	56.05	1.6400	1.6394	7	w
3	3	1	57.19	1.6090	1.6094	23	m
2	2	2	60.22	1.5352	1.5355	8	w
3	1	2	62.93	1.4755	1.4756	26	m
3	2	2	66.90	1.3977	1.3974	3	vw
5	1	1	67.97	1.3783	1.3780	18	w

Note. Visual intensities are given in units of vs (very strong), s (strong), m (medium), w (weak), and vw (very weak). Calculated intensities were generated with Lazy-Pulverix (22).

TABLE 2
Crystal Data and Structure Refinement for Ce_2Ni_2Cd

Empirical formula	Ce_2Ni_2Cd
Molar mass (g/mol)	510.06
Space group, Z	$P4/mbm$, 2
Pearson symbol	tP10
Unit cell dimensions	$a = 755.67(8)$ pm
(Guinier powder data)	$c = 375.14(6)$ pm
	$V = 0.2142(1)$ nm^3
Calculated density (g/cm^3)	7.91
Crystal size (μm^3)	$15 \times 20 \times 30$
Transmission ratio (max/min)	1.17
Absorption coefficient (mm^{-1})	34.1
$F(000)$	440
θ range for data collection	2°–32°
Range in hkl	± 11, ± 11, $+5$
Total no. of reflections	1585
Independent reflections	232 ($R_{int} = 0.0678$)
Reflections with $I > 2\sigma(I)$	183 ($R_{sigma} = 0.0320$)
Data/restraints/parameters	232/0/13
Goodness-of-fit on F^2	1.134
Final R indices [$I > 2\sigma(I)$]	$R1 = 0.0176$; w$R2 = 0.0351$
R indices (all data)	$R1 = 0.0384$; w$R2 = 0.0408$
Extinction coefficient	0.0059(6)
Largest diff. peak and hole	2.00 and -1.76 e/Å^3

The magnetic susceptibilities of polycrystalline pieces of Ce_2Ni_2Cd were measured with a SQUID magnetometer (MPMS, Quantum Design, Inc.) between 2 and 300 K with magnetic flux densities up to 5 T. Resistivity measurements were performed with a conventional four-point technique. Four copper filaments were glued to the irregularly shaped samples (typical dimensions $1 \times 1 \times 1$ mm^3) using a well-conducting silver epoxy paste. Cooling and heating curves were identical within the error limits.

RESULTS AND DISCUSSION

Structure Refinement

Irregularly shaped single crystals of Ce_2Ni_2Cd were isolated from the annealed samples and examined by use of a Buerger camera. The precession photographs showed

Single-crystal intensity data were collected at room temperature by use of a four-circle diffractometer (CAD4) with graphite monochromatized Mo$K\alpha$ (71.073 pm) radiation and a scintillation counter with pulse height discrimination. The scans were taken in the $\omega/2\theta$ mode and an empirical absorption correction was applied on the basis of psi-scan data.

TABLE 3
Atomic Coordinates and Isotropic Displacement Parameters (pm^2) for Ce_2Ni_2Cd

Atom	Wyckoff site	Occup.	x	y	z	U_{eq}
Ce	4*h*	1.00	0.17428(5)	$1/2+x$	1/2	115(2)
Ni	4*g*	0.940(6)	0.3788(1)	$1/2+x$	0	187(5)
Cd	2*a*	1.00	0	0	0	145(2)

Note. U_{eq} is defined as one-third of the trace of the orthogonalized U_{ij} tensor.

TABLE 4
Interatomic Distances (pm), Calculated with the Lattice Constants Taken from X-ray Powder Data of Ce_2Ni_2Cd

Ce:	2	Ni	288.0(1)	Ni:	1	Ni	259.1(3)
	4	Ni	294.4(1)		2	Ce	288.0(1)
	4	Cd	336.3(1)		4	Ce	294.4(1)
	1	Ce	372.5(1)		2	Cd	300.5(1)
	2	Ce	375.1(1)				
	4	Ce	394.8(1)	Cd:	4	Ni	300.5(1)
					8	Ce	336.3(1)

Note. All distances shorter than 510 pm (Ce–Ce, Ce–Ni, Ce–Cd), 475 pm (Ni–Cd), and 370 pm (Ni–Ni, Cd–Cd) are listed.

a primitive tetragonal cell. The systematic extinctions were compatible with space group $P4/mbm$ in agreement with our previous results on Ce_2Pt_2In (23). The powder pattern and the single-crystal data gave no indication for a unit cell doubling (superstructure of the Er_2Au_2Sn type), as frequently observed for this family of compounds (16–18, 24). All relevant crystallographic data and experimental details for the data collection are listed in Table 2.

The atomic parameters of Ce_2Pt_2In (23) were taken as starting values and the structure was sucessfully refined using SHELXL-97 (25) (full-matrix least-squares on F^2) with anisotropic atomic displacement parameters for all atoms. During the refinement procedure, the equivalent isotropic displacement parameter of the nickel site was somewhat elevated (234(5) pm^2), indicating defects on this position, since the nickel atoms have the smallest scattering power in this compound. As a check for the correct site assignment, the occupancy parameters were refined in a separate series of least-squares cycles along with the displacement parameters. No deviation from full occupancy was observed for the cerium and cadmium site, while some defects occurred for the nickel site. In the final cycles the ideal occupancy parameters were assumed for cerium and cadmium, while the occupancy parameter of the nickel site was allowed to vary. The refinement then readily converged to the residuals listed in Table 2 and the composition was $Ce_2Ni_{1.88(1)}Cd$ for the crystal investigated. A final difference Fourier synthesis was flat (Table 2). The positional parameters and interatomic distances of the refinements are listed in Tables 3 and 4. Listings of the observed and calculated structure factors are available.[2]

Crystal Chemistry and Chemical Bonding

Ce_2Ni_2Cd is the first cadmium compound in the series of tetragonal R_2T_2X intermetallics. A projection of the Ce_2Ni_2Cd structure is shown in Fig. 1. From a geometrical point of view it is built up from distorted AlB_2- and CsCl-related slabs of compositions *CeNi*$_2$ and *CeCd*, respectively, as emphasized at the right-hand part of Fig. 1. While a high-temperature (HT) modification of CeCd with a CsCl-type structure is known (26), $CeNi_2$ (27) adopts the structure of the cubic Laves phase $MgCu_2$. In HT-CeCd the Ce–Cd distance is 333.5 pm. At low temperatures a tetragonal distortion to LT-CeCd occurs with a c/a ratio of 1.03 and Ce–Cd distances of 332.4 pm (26). In contrast, the c/a ratio in the compressed *CeCd* slab of Ce_2Ni_2Cd is 0.95 and the Ce–Cd distances of 336.3 pm are slightly longer.

The Ce–Ni distances within the distorted AlB_2 slab of 288.0 and 294.4 pm are shorter than those in the $CeNi_{12}$ icosahedron of $CeNi_2$ (298.8 pm) with $MgCu_2$-type structure (27). They are only somewhat larger than the sum of

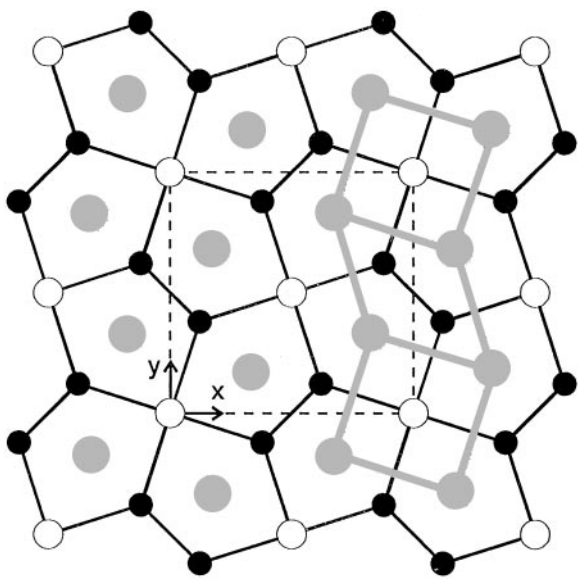

FIG. 1. Projection of the Ce_2Ni_2Cd structure onto the *xy plane*. Cerium, nickel, and cadmium atoms are drawn as gray, black-filled, and black open circles, respectively. The two-dimensional $[Ni_2Cd]$ network at $z = 0$ as well as the trigonal and square prismatic cerium slabs at $z = \frac{1}{2}$ are emphasized.

[2] Details may be obtained from: Fachinformationszentrum Karlsruhe, D-76344 Eggenstein-Leopholdshafen (Germany), by quoting the Registry No. CSD-410937.

Pauling's single-bond radii (28) of 280 pm for cerium and nickel. Thus, one may assume a significant degree of Ce–Ni bonding in Ce_2Ni_2Cd. This is in good agreement with a recent extended Hückel band structure investigation of isotypic Sc_2Ni_2In (4). Here, the strongest bonding interactions were found for the Sc–Ni contacts, followed by Sc–In and Ni–In. This model of chemical bonding can safely be applied also to Ce_2Ni_2Cd. The electron count of Ce_2Ni_2Cd is only slightly lower than that for Sc_2Ni_2In. Assuming a rigid band model, the Fermi level is only slightly decreased.

The Ni–Ni distance of 259.1 pm within the distorted AlB_2 slab is longer than the Ni-Ni distance of 249.2 pm in fcc nickel (29). In Sc_2Ni_2In (4) and Zr_2Ni_2Sn (11) with the smaller scandium, respectively zirconium atoms, Ni–Ni distances of 251.6 and 250.6 pm were observed. Within the two-dimensional $[Ni_2Cd]$ network at $z = 0$ each cadmium atom has a square planar nickel coordination with Ni-Cd distances of 300.5 pm, much longer than the sum of Pauling's single-bond radii (28) of 256.7 pm for nickel and cadmium. Also, in the structure of NiCd (30) relatively long Ni–Cd distances of 286 pm occur.

The structure refinement revealed small defects on the nickel site. The refined composition of the investigated single crystal was $Ce_2Ni_{1.88(1)}Cd$. A small homogeneity range of $Ce_2Ni_{2-x}Cd$ is possible, but it was not studied in detail. The refined nickel occupancy may slightly vary from crystal to crystal. EDX analyses (see above) of the bulk sample did not show such defects. Within the error limits of these analyses, the sample is homogenous and of the intended composition Ce_2Ni_2Cd. The physical properties reported below refer to this sample. The formation of small defects was also observed for the $Ln_2Ni_{2-x}In$ compounds with Ln = Y, Sm, Gd–Tm, Lu (31); however, these compounds crystallize with the orthorhombic Mn_2AlB_2 type (32), while those with the exact 2:2:1 composition crystallize with the tetragonal Mo_2FeB_2 type, as Ce_2Ni_2Cd does. Very recently, Canepa and co-workers reported on antiferromagnetic Gd_2Ni_2Cd (33) with a Mn_2AlB_2-type structure. Most likely, the Ln_2T_2Cd compounds with the light rare earth metals form the tetragonal Mo_2FeB_2 type, while those with the heavy rare earth atoms adopt the orthorhombic Mn_2AlB_2 type.

Magnetic and Electrical Properties

The temperature dependence of the inverse magnetic susceptibility of Ce_2Ni_2Cd is displayed in Fig. 1. The susceptibilities were only weakly dependent on the external magnetic field, indicating only minor amounts of ferromagnetic impurities. The data measured at 1 and 3 T were almost identical and we have plotted the 3-T data in Fig. 2. The strong variation of the reciprocal susceptibility vs temperature is not compatible with Curie–Weiss behavior.

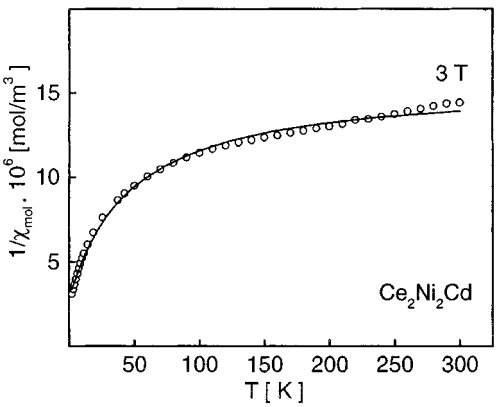

FIG. 2. Temperature dependence of the inverse magnetic susceptibility of Ce_2Ni_2Cd. The solid line corresponds to the least-squares fit of the data according to a modified Curie–Weiss expression (see text).

A naive evaluation of the data above 150 K according to the Curie–Weiss law results in an almost infinite magnetic moment and a strongly negative paramagnetic Curie temperature (Weiss constant) of -700 ± 30 K. Both of these features are indicative of a valence fluctuation system. We have thus fitted the susceptibility with a modified Curie–Weiss expression $\chi = \chi_0 + C/(T - \Theta_P)$, where Θ_P is the asymptotic paramagnetic Curie temperature and χ_0 includes the temperature-independent Van Vleck correction, the core diamagnetism, and the paramagnetic contribution of the conduction electrons (Pauli contribution). A least-squares fit yielded a small experimental magnetic moment, $\mu_{exp} = 0.79(3)\ \mu_B$/Ce, a slightly negative paramagnetic Curie temperature $\Theta_P = -5.2(2)$ K and $\chi_0 = 67.5(7) \times 10^{-9}$ m^3/mol. The rather small experimental moment corresponds to the delocalized nature of the 4*f* electrons in accordance with a nearly tetravalent state of the cerium atoms. For trivalent cerium a magnetic moment near $\mu_{calc} = 2.54\ \mu_B$/Ce would occur.

The magnetization vs external field dependence at 2 and 50 K is presented in Fig. 3. The experimental

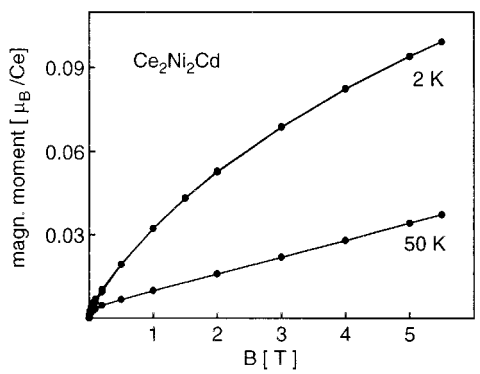

FIG. 3. Magnetization vs external magnetic flux density for Ce_2Ni_2Cd at 2 and 50 K.

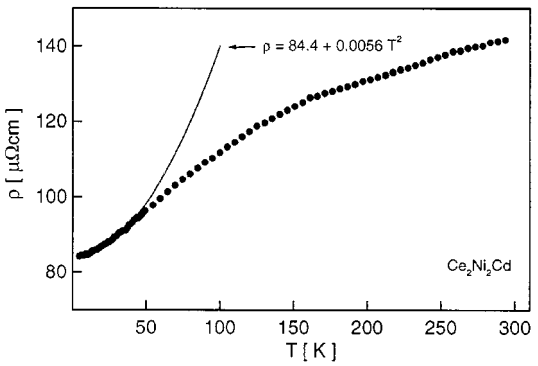

FIG. 4. Temperature dependence of the specific resistivity of Ce_2Ni_2Cd. The solid line marks a T^2 variation of the specific resistivity at low temperatures.

magnetizations of 0.04 μ_B/Ce (50 K) and 0.10 μ_B/Ce (2 K) at the highest obtainable field of 5.5 T are extremely small, in agreement with the intermediate-valent behavior discussed above. Similar intermediate-valent behavior was observed recently also for isotypic Ce_2Ni_2In and Ce_2Rh_2In (6) as well as for the equiatomic compounds CeRhIn (34), CeNiIn (35), CeRhSb (36), CeNiSn (37), and CeIrGe (38). Also the silicides CeT_2Si_2 (T = Ru, Pd, Os, Ir, Pt) show a nonmagnetic cerium ground state (39, 40).

In Fig. 4 we display the temperature dependence of the specific resistivity. The latter decreases with decreasing temperature, indicating metallic behavior. At room temperature the specific resistivity has a value of 140 ± 20 μΩ cm and the resistivity ratio $\rho(4.2\text{ K})/\rho(300\text{ K})$ is about 0.6. The error limit of 20 μΩ cm accounts for the values obtained for different samples. This is most likely due to the brittleness and microcracks in the well-crystallized sample.

Ce_2Ni_2Cd shows the resistivity behavior of an intermediate-valence material (41). According to the paramagnon picture of such systems, their specific resistivity at low temperature should reveal a T^2 dependence characteristic of a Fermi liquid (42). As shown in Fig. 4, the specific resistivity of Ce_2Ni_2Cd can be well described below 50 K by the formula $\rho(T) = \rho_0 + AT^2$. A least-squares fit resulted in the values $\rho_0 = 84.4(1)$ μΩ cm and $A = 0.0056(1)$ (μΩ cm)/K^2. The uncertainty of the absolute values of the specific resistivity discussed above, however, hampered any further quantitative discussion of the electrical behavior of Ce_2Ni_2Cd. The large negative curvature of the ρ vs T plot above 50 K can be interpreted in terms of a spin-scattering mechanism in the intermediate-valent regime (41). Similar resistivity data have recently also been observed for isotypic Ce_2Ni_2In and Ce_2Rh_2In (6) as well as for CeRhIn (34) and $CeIr_2Si_2$ (40).

In summary, we have synthesized Ce_2Ni_2Cd, the first cadmium compound in the series of Ce_2T_2X intermetallics. Metallic Ce_2Ni_2Cd crystallizes with an ordered U_3Si_2-type structure and may be classified as a new valence fluctuating system. Detailed investigations on other Ce_2T_2Cd compounds with promosing physical properties are now in progress.

ACKNOWLEDGMENTS

We are grateful to Prof. W. Jeitschko for his interest and steady support. We are also indebted to Dipl.-Ing. U. Ch. Rodewald for the intensity data collection and to K. Wagner for the EDX analyses. This work was financially supported by the Bennigsen-Foerder-Programm of the Ministerium für Wissenschaft und Forschung des Landes Nordrhein-Westfalen, by the Fonds der Chemischen Industrie and the Deutsche Forschungsgemeinschaft.

REFERENCES

1. F. Mirambet, P. Gravereau, B. Chevalier, L. Trut, and J. Etourneau, *J. Alloys Compd.* **191,** L1 (1993).
2. M. N. Peron, Y. Kergadallan, J. Rebizant, D. Meyer, J. M. Winand, S. Zwirner, L. Havela, H. Nakotte, J. C. Spirlet, G. M. Kalvius, E. Colineau, J. L. Oddou, C. Jeandey, and J. P. Sanchez, *J. Alloys Compd.* **201,** 203 (1993).
3. F. Mirambet, B. Chevalier, L. Fournès, P. Gravereau, and J. Etourneau, *J. Alloys Compd.* **203,** 29 (1994).
4. R. Pöttgen and R. Dronskowski, *Z. Anorg. Allg. Chem.* **622,** 355 (1996).
5. H. Nakotte, A. Purwanto, R. A. Robinson, K. Prokeš, J. C. P. Klaasse, P. F. de Châtel, F. R. de Boer, L. Havela, V. Sechovký, L. C. J. Pereira, A. Seret, J. Rebizant, J. C. Spirlet, and F. Trouw, *Phys. Rev. B* **53,** 3263 (1996).
6. D. Kaczorowski, R. Rogl, and K. Hiebl, *Phys. Rev. B* **54,** 9891 (1996).
7. M. Giovannini, H. Michor, E. Bauer, G. Hilscher, P. Rogl, and R. Ferro, *J. Alloys Compd.* **280,** 26 (1998).
8. M. Diviš, M. Olšovec, M. Richter, and H. Eschrig, *J. Magn. Magn. Mater.* **140–144,** 1365 (1995).
9. K. Prokeš, E. Brück, H. Nakotte, P. F. de Châtel, and F. R. de Boer, *Physica B* **206/207,** 8 (1995).
10. S. F. Matar, *J. Magn. Magn. Mater.* **151,** 263 (1995).
11. R. Pöttgen and R. Dronskowski, *J. Solid State Chem.* **128,** 289 (1997).
12. L. Havela, V. Sechovký, P. Svoboda, M. Diviš, H. Nakotte, K. Prokeš, F. R. de Boer, A. Purwanto, R. A. Robinson, A. Seret, J. M. Winand, J. Rebizant, J. C. Spirlet, M. Richter, and H. Eschrig, *J. Appl. Phys.* **76,** 6214 (1994).
13. W. Rieger, H. Nowotny, and F. Benesovsky, *Monatsh. Chem.* **95,** 1502 (1964).
14. W. H. Zachariasen, *Acta Crystallogr.* **2,** 94 (1949).
15. K. Remschnig, T. Le Bihan, H. Noël, and P. Rogl, *J. Solid State Chem.* **97,** 391 (1992).
16. R. Pöttgen, *Z. Naturforsch. B* **49,** 1309 (1994).
17. P. Gravereau, F. Mirambet, B. Chevalier, F. Weill, L. Fournès, D. Laffargue, F. Bourrée, and J. Etourneau, *J. Mater. Chem.* **4,** 1893 (1994).
18. M. F. Zumdick, R. Pöttgen, R. Müllmann, B. D. Mosel, G. Kotzyba, and B. Künnen, *Z. Anorg. Allg. Chem.* **624,** 251 (1998).
19. C. G. Wilson and F. J. Spooner, *Acta Crystallogr.* **13,** 358 (1960).
20. R. Pöttgen, Th. Gulden, and A. Simon, *GIT-Laborfachzeitschrift* **43,** 133 (1999).
21. R. Pöttgen, A. Lang, R.-D. Hoffmann, B. Künnen, G. Kotzyba, R. Müllmann, B. D. Mosel, and C. Rosenhahn, *Z. Kristallogr.* **214,** 143 (1999).
22. K. Yvon, W. Jeitschko, and E. Parthé, *J. Appl. Crystallogr.* **10,** 73 (1977).
23. Ya. V. Galadzhun and R. Pöttgen, *Z. Anorg. Allg. Chem.* **625,** 481 (1999).

24. R. Pöttgen, P. E. Arpe, C. Felser, D. Kußmann, R. Müllmann, B. D. Mosel, B. Künnen, and G. Kotzyba, *J. Solid State Chem.* **145,** 668 (1999).
25. G. M. Sheldrick, "SHELXL-97, Program for Crystal Structure Refinement," University of Göttingen, 1997.
26. M. Nakazatro, N. Wakabayashi, and T. Kitai, *J. Phys. Soc. Jpn.* **57,** 953 (1988).
27. T. C. Shields, J. Mayers, and I. R. Harris, *J. Magn. Magn. Mater.* **63/64,** 587 (1987).
28. L. Pauling, "The Nature of the Chemical Bond and The Structures of Molecules and Crystals." Cornell University Press, Ithaca, NY, 1960.
29. J. Donohue, "The Structures of the Elements." Wiley, New York, 1974.
30. J. K. Critchley and J. W. Jeffery, *Acta Crystallogr.* **19,** 674 (1965).
31. Ya. M. Kalychak, V. I. Zaremba, V. M. Baranyak, P. Yu. Zavalii, V. A. Bruskov, L. V. Sysa, and O. V. Dmytrakh, *Inorg. Mater.* **26,** 74 (1990).
32. H. J. Becher, K. Krogmann, and E. Peisker, *Z. Anorg. Allg. Chem.* **344,** 140 (1966).
33. F. Canepa, S. Cirafici, F. Merlo, M. Pani, and C. Ferdeghini, *J. Magn. Magn. Mater.* **195,** 646 (1999).
34. D. T. Adroja, S. K. Malik, B. D. Padalia, and R. Vijayaraghavan, *Phys. Rev. B* **39,** 4831 (1989).
35. K. Satoh, T. Fujita, Y. Maeno, Y. Uwatoko, and H. Fujii, *J. Phys. Soc. Jpn.* **59,** 692 (1990).
36. S. K. Malik and D. T. Adroja, *Phys. Rev. B* **43,** 6277 (1991).
37. T. Takabatake, F. Teshima, H. Fujii, S. Nishigori, T. Suzuki, T. Fujita, Y. Yamaguchi, J. Sakurai, and D. Jaccard, *Phys. Rev. B* **41,** 9607 (1990).
38. P. Rogl, B. Chevalier, M. J. Besnus, and J. Etourneau, *J. Magn. Magn. Mater.* **80,** 305 (1989).
39. K. Hiebl, C. Horvath, and P. Rogl, *J. Less-Common Met.* **117,** 375 (1986).
40. B. Buffat, B. Chevalier, M. H. Tuilier, B. Lloret, and J. Etourneau, *Solid State Commun.* **59,** 17 (1986).
41. D. Wohlleben and B. Wittershagen, *Adv. Phys.* **34,** 403 (1985).
42. J. M. Lawrence, P. S. Riseborough, and R. D. Parks, *Rep. Prog. Phys.* **44,** 1 (1981).